3-30-2012

Piceatannol, Natural Polyphenolic Stilbene, Inhibits Adipogenesis via Modulation of Mitotic Clonal Expansion and Insulin Receptor-dependent Insulin Signaling in Early Phase of Differentiation

Jung Yeon Kwon
Purdue University

Sang Gwon Seo
Seoul National University

Yong-Seok Heo
Konkuk University

Shuhua Yue
Purdue University

Ji-Xin Cheng
Purdue University

See next page for additional authors

Recommended Citation

Kwon JY, Seo SG, Heo YS, Yue S, Cheng JX, Lee KW, Kim KH. Piceatannol, natural polyphenolic stilbene, inhibits adipogenesis via modulation of mitotic clonal expansion and insulin receptor-dependent insulin signaling in early phase of differentiation. J Biol Chem. 2012 Mar 30;287(14):11566-78. doi: 10.1074/jbc.M111.259721.

THE JOURNAL OF BIOLOGICAL CHEMISTRY VOL. 287, NO. 14, pp. 11566–11578, March 30, 2012

Piceatannol, Natural Polyphenolic Stilbene, Inhibits Adipogenesis via Modulation of Mitotic Clonal Expansion and Insulin Receptor-dependent Insulin Signaling in Early Phase of Differentiation*

Received for publication, May 10, 2011, and in revised form, January 26, 2012 Published, JBC Papers in Press, January 31, 2012, DOI 10.1074/jbc.M111.259721

Jung Yeon Kwon[‡], Sang Gwon Seo[§], Yong-Seok Heo[¶], Shuhua Yue[‖], Ji-Xin Cheng[‖], Ki Won Lee[§], and Kee-Hong Kim[‡1]**

*From the [‡]Department of Food Science, Purdue University, West Lafayette, Indiana 47907, the [§]Department of Agricultural Biotechnology, Seoul National University, Seoul 151-921, Republic of Korea, the [¶]Department of Chemistry, Konkuk University, Seoul 143-701, Republic of Korea, and the [‖]Weldon School of Biomedical Engineering and the **Department of Chemistry, Purdue University, West Lafayette, Indiana 47907*

Background: Adipogenesis contributes to the increase in adipose tissue mass.
Results: Preadipocytes treated with piceatannol showed reduced adipogenesis with impairment of the early cell cycle progress and insulin-signaling pathway.
Conclusion: The anti-adipogenic function of piceatannol is through inhibition of mitotic clonal expansion and insulin receptor activity in the early phase of adipogenesis.
Significance: Piceatannol is a novel anti-adipogenic compound that could modulate development of adipose tissue.

Piceatannol, a natural stilbene, is an analog and a metabolite of resveratrol. Despite a well documented health benefit of resveratrol in intervention of the development of obesity, the role of piceatannol in the development of adipose tissue and related diseases is unknown. Here, we sought to determine the function of piceatannol in adipogenesis and elucidate the underlying mechanism. We show that piceatannol inhibits adipogenesis of 3T3-L1 preadipocytes in a dose-dependent manner at noncytotoxic concentrations. This anti-adipogenic property of piceatannol was largely limited to the early event of adipogenesis. In the early phase of adipogenesis, piceatannol-treated preadipocytes displayed a delayed cell cycle entry into G_2/M phase at 24 h after initiation of adipogenesis. Furthermore, the piceatannol-suppressed mitotic clonal expansion was accompanied by reduced activation of the insulin-signaling pathway. Piceatannol dose-dependently inhibited differentiation mixture-induced phosphorylation of insulin receptor (IR)/insulin receptor substrate-1 (IRS-1)/Akt pathway in the early phase of adipogenesis. Moreover, we showed that piceatannol is an inhibitor of IR kinase activity and phosphatidylinositol 3-kinase (PI3K). Our kinetics study of IR further identified a K_m value for ATP of 57.8 μM and a K_i value for piceatannol of 28.9 μM. We also showed that piceatannol directly binds to IR and inhibits IR kinase activity in a mixed noncompetitive manner to ATP, through which piceatannol appears to inhibit adipogenesis. Taken together, our study reveals an anti-adipogenic function of piceatannol and highlights IR and its downstream insulin signaling as novel targets for piceatannol in the early phase of adipogenesis.

Obesity is a global health concern, and it is caused by many factors, including overnutrition and lack of physical activity. Excess storage of lipids in adipose tissue is the key feature of obesity, which is associated with type 2 diabetes and cardiovascular disease (1). Both adipocytes hyperplasia and adipocytes hypertrophy are determinant factors for adipose mass increase. Adipogenesis is responsible for adipocyte hyperplasia, and it also contributes to a compensatory replacement of adipocyte loss due to an active adipocyte turnover in adipose tissue in adult humans (2). The molecular and cellular process of adipogenesis has been extensively characterized using preadipocyte clonal cell lines (*e.g.* 3T3-L1 and 3T3-F442A) (3, 4). Adipogenesis requires a concerted transcriptional and cellular program, including growth arrest of confluent preadipocytes, reentry to the cell cycle for an additional two rounds of division, termed mitotic clonal expansion (MCE),[2] and the initiation of transcriptional events in the early and late phases of differentiation (3). Among factors promoting adipogenesis, adipogenic transcription factors such as CCAAT/enhancer-binding protein β (C/EBPβ), peroxisome proliferator-activated receptor γ (PPARγ), and C/EBPα, and cellular signaling cascades involved in cell cycle and insulin-dependent signaling pathways in the early phase of adipogenesis are known to play critical roles (4, 5). In particular, insulin- and insulin-like growth factor-1 (IGF-

* This work was supported in part by a Purdue Research Foundation grant (to K. H. K.) and in part by National Research Foundation and Ministry of Education, Science, and Technology, Republic of Korea, Leap Research Program Grants 2010-0029233 and 2009-0067326 (to K. W. L.).
[1] To whom correspondence should be addressed: Dept. of Food Science, Purdue University, West Lafayette, IN 47907. Tel.: 765-496-2330; Fax: 765-494-7953; E-mail: keehong@purdue.edu.

[2] The abbreviations used are: MCE, mitotic clonal expansion; C/EBP, CCAAT/enhancer-binding protein; PPARγ, peroxisome proliferator-activated receptor γ; IR, insulin receptor; Syk, spleen tyrosine kinase; NF-κB, nuclear factor-κB; DMI, dexamethasone, 3-isobutyl-1-methylxanthine, insulin; CARS, multimodal coherent anti-Stokes Raman scattering; MTT, 3-(4,5-dimethylthiazol-2-yl)-2,5-diphenyltetrazolium bromide.

1)-activated PI3K/Akt pathway and the mitogen-activated protein kinase/extracellular signal-regulated kinase (MAPK/ERK) pathway are known to play a key role in adipogenesis (6–10). This appears to be through sensing cell cycle progression in MCE and phosphorylation of transcriptional activation of C/EBPβ for its subsequent transcriptional activation of PPARγ and C/EBPα (11–13). Disruption of the insulin receptor (IR) gene *in vitro* and *in vivo* resulted in impaired adipogenesis and adipose development, respectively (14, 15). Ablation of insulin receptor substrate-1 (IRS-1) and IRS-3 or inactivation of PI3K/Akt pathways inhibited adipogenesis (16, 17).

Piceatannol (*trans*-3,4,3′,5′-tetrahydroxystilbene) is a natural polyphenolic stilbene present in grapes, red wine (18), and *Euphorbia lagascae* seeds (19). It is suggested to have anti-cancer and anti-inflammatory properties (20–22), and this beneficial impact may stem from its inhibitory effects on various kinase activities, including spleen tyrosine kinase (Syk) and PI3K, and nuclear factor-κB-mediated gene expression (22, 23). Piceatannol is a natural analog and a metabolite of resveratrol having an extra hydroxyl group at the 3′ position. Increasing evidence implicates a health-promoting and therapeutic effect of resveratrol on aging and chronic diseases such as obesity (24, 25). However, poor bioavailability and rapid metabolism limit the use of resveratrol in dietary intervention for these diseases. This posits that hydroxylated resveratrol metabolites, such as piceatannol, may be an alternative to resveratrol for a benefit to the health. However, the potential role of piceatannol in adipose tissue development and obesity and its underlying mechanisms have not yet been studied.

In this study, we have investigated a potential role of piceatannol in regulating adipogenesis of 3T3-L1 preadipocytes. We show that piceatannol inhibits adipogenesis with no effect on the viability of the differentiating preadipocytes. This anti-adipogenic function targets the MCE phase, where piceatannol suppresses cell cycle progression and expression of pro-adipogenic transcription factors, C/EBPβ, PPARγ, and C/EBPα. The piceatannol-associated blockage of MCE phase is accompanied by an inhibition of phosphorylation and kinase activity of IR and its mediated PI3K/Akt signaling pathway. Moreover, our pulldown assay using piceatannol-conjugated beads elucidates that piceatannol directly binds to IR in an ATP-noncompetitive manner. Taken together, these data show that piceatannol is a natural anti-adipogenic small molecule that inhibits MCE phase and IR-mediated insulin-signaling pathway in the early phase of adipogenesis.

EXPERIMENTAL PROCEDURES

Materials and Reagents—Piceatannol was purchased from Alexis Biochemicals (Lausen, Switzerland). Dexamethasone, 3-isobutyl-1-methylxanthine, insulin, propidium iodide, and RNase A were obtained from Sigma. Fetal calf serum (FCS) and fetal bovine serum (FBS) were purchased from PAA (Dartmouth, MA). Dulbecco's modified Eagle's medium (DMEM), penicillin/streptomycin, sodium pyruvate, TRIzol® reagent, and SuperScriptII kit were obtained from Invitrogen. 3-(4,5-Dimethylthiazol-2-yl)-2,5-diphenyltetrazolium bromide (MTT) was purchased from Alfa Aesar (Ward Hill, MA). Protein assay kit was obtained from Bio-Rad. Antibodies against C/EBPα, C/EBPβ, phospho-IRβ (Tyr(P)-1146), and phospho-ERK1/2 were obtained from Cell Signaling Biotechnology (Beverly, MA). Antibodies against phospho-Akt (Ser(P)-473) and Akt were purchased from Epitomics (Burlingame, CA). Antibody against phosphotyrosine was purchased from MP Biomedicals (Solon, OH). Antibodies against PPARγ, His probe (H-3), β-actin, and rabbit and mouse secondary were purchased from Santa Cruz Biotechnology (Santa Cruz, CA). [γ-^{32}P]ATP and CNBr-Sepharose 4B were obtained from Amersham Biosciences. PI3K (a complex of N-terminal His_6-tagged recombinant human p110δ and untagged recombinant human p85α) and IR active protein (N-terminal His_6-tagged recombinant human protein with residues 1005–1310) were purchased from Millipore (Billerica, MA), and IRS-1-derived peptide was obtained from Anaspec (Fremont, CA).

Cell Culture and Differentiation—3T3-L1 preadipocytes were obtained from American Type Culture Collection and maintained in DMEM containing 10% (v/v) FCS in a humidified atmosphere of 5% CO_2 at 37 °C. The cells were induced to differentiate on reaching 2-day postconfluency (designated as day 0) by supplementation of standard adipogenic mixture, including 5 μM dexamethasone, 0.5 mM 3-isobutyl-1-methylxanthine, and 167 nM insulin (DMI) in 10% FBS/DMEM for 2 days. The medium was changed to 10% FBS/DMEM containing insulin on day 2 and to 10% FBS/DMEM on day 4. On day 6, cells were subjected to Oil Red O staining to visualize accumulated lipid droplets in the cells. Intracellular lipid content was quantified by extracting Oil Red O by isopropyl alcohol and measuring the absorbance at 490 nm by a spectrophotometer.

Multimodal Coherent Anti-Stokes Raman Scattering (CARS) Microscope—A multimodal microscope capable of simultaneous CARS and two-photon excitation fluorescence imaging analysis was performed as described previously (26). Briefly, for CARS imaging of lipid droplets in adipocytes, the wave number difference between the pump laser and Stokes laser tuned to 2840 cm^{-1}, which matches the Raman shift of the symmetric CH_2 stretch vibration in lipid molecules. Combined beams were focused into the specimen through a 60× water immersion objective with a 1.2 numerical aperture. The forward CARS signal was collected by an air condenser (numerical aperture = 0.55), transmitted through a 600/65-nm bandpass filter and detected by a photomultiplier tube (H7422-40, Hamamatsu, Japan). For and two-photon excitation fluorescence imaging of intracellular fluorescent piceatannol, the backward signal was collected by the objective, spectrally separated from the excitation source, transmitted through a 520/40-nm bandpass filter, and detected by a photomultiplier tube mounted at the back port of the microscope. The combined pump and Stokes laser power at the specimen was kept constant at 55 milliwatts. Acquisition time for each image was 1.12 s. Images were analyzed using Fluo-View software (Olympus, PA).

Immunoblot Assay—The cells were cultured and treated as indicated in each experiment and harvested by scraping in cell lysis buffer containing Tris-HCl (100 mM (pH 8.0)), NaCl (100 mM), 0.5% Triton X-100, protease inhibitor mixture, sodium orthovanadate (1 mM), and sodium fluoride (10 mM). Protein concentration was determined protein assay kit (Bio-Rad). Pro-

teins were separated on a SDS-polyacrylamide gel and transferred to nitrocellulose membrane. Immunoblot was performed with the respective primary antibodies and horseradish peroxidase-conjugated secondary antibodies (Santa Cruz Biotechnology). Signals were visualized by enhanced chemiluminescence kit (Pierce).

Cell Viability Assay—The cells were treated with DMI and various concentrations of piceatannol for 48 h. Subsequent incubation of the cells with MTT solution (0.5 mg/ml) for 1 h at 37 °C allowed formation of a violet precipitate, formazan. It was dissolved in DMSO, and the absorbance was measured at 595 nm on a microplate reader (Beckman-Coulter).

Isolation of Total RNA and Real Time Reverse Transcription (RT)-PCR—Total RNA in the cells was extracted using TRIzol® reagent as described in the manufacturer's instructions. 1 μg/μl isolated total RNA was used to synthesize cDNA by SuperScriptII kit, and real time PCR was performed to amplify cDNA. For real time PCR, cDNA was diluted and mixed with SYBR premixed Taq reaction mixture (Applied Biosystems) containing 100 ng/ml PCR primers. Reactions were performed in triplicate for each pair of primers using StepOne real time PCR system (Applied Biosystems). The sequences of primers used in the reactions are as follows: C/EBPβ (forward, 5′-GCA AGA GCC GCG ACA AG-3′, and reverse, 5′-GGC TCG GGC AGC TGC TT-3′); PPARγ (forward, 5′-CCA CCA ACT TCG GAA TCA GCT-3′, and reverse, 5′-TTT GTG GAT CCG GCA GTT AAG A-3′); C/EBPα (forward, 5′-GCT GGA GTT GAC CAG TGA CA-3′, and reverse, 5′-AAA CCA TCC TCT GGG TCT CC-3′); β-actin (forward, 5′-TGA CGG GGT CAC CCA CAC TGT GCC CAT CTA-3′, and reverse, 5′-CTA GAA GCA TTT GCG GTG GAC GAT GGA GGG-3′).

Cell Cycle Analysis—The cells were collected at the indicated time points after stimulation with DMI in the absence or presence of piceatannol. Harvested cells were fixed with 70% ethanol for 2 h on ice, washed twice with PBS, and stained with 40 μg/ml propidium iodine solution containing 500 μg/ml of RNase A for 30 min at 37 °C. Cell cycle analysis was performed using a Cell Lab Quanta SC flow cytometer (Beckman-Coulter) according to the manufacturer's manual.

PI3K Assay—In vitro kinase assays were performed as described previously (23). Briefly, active PI3K protein (100 ng) was incubated with different concentrations of piceatannol or LY294002, a PI3K inhibitor, at 30 °C for 10 min. Following the incubation with 20 μl of 0.5 mg/ml phosphatidylinositol (Avanti Polar Lipids), the mixture was incubated with the reaction buffer (100 mM HEPES (pH 7.6), 50 mM $MgCl_2$, and 250 μM ATP containing 10 μCi of [γ-^{32}P]ATP) for an additional 10 min and finally with the stopping buffer (15 μl of 4 N HCl and 130 μl of chloroform/methanol, 1:1). A 1% potassium oxalate-coated silica gel plate (Merck), which was previously activated for 1 h at 110 °C, was used to spot the lower chloroform phase in the mixture. Thin layer chromatography was used to separate the resulting ^{32}P-labeled phosphatidylinositol 3-phosphate, and autoradiography was used to visualize the radiolabeled spots.

IR Kinase Assay—Briefly, purified active recombinant human IR with a final concentration of 1.3 nM was incubated with reaction buffer (8 mM MOPS (pH 7.0), 0.2 mM EDTA, 1 mM Na_3VO_4, 5 mM sodium-β-glycerophosphate, 500 μM synthetic peptide (KKKSPGEYVNIEFG), 10 mM magnesium acetate, and [γ-^{33}P]ATP). Mg-ATP mixture was added to initiate the reaction. Following a 40-min incubation at room temperature, 3% phosphoric acid solution was added to stop the reaction. 10 μl of reaction mixture was spotted onto a P30 filter paper. After washing three times in 75 mM phosphoric acid and once in methanol, it was dried and subjected for scintillation counting. The ATP concentrations used in the assay were 5, 25, 45, 90, 200, and 500 μM, and the activity of IR at each ATP concentration was determined at different concentrations of piceatannol. All data were performed in duplicate. Michaelis-Menten constant (K_m) and maximum activity (V_{max}), the half-maximal inhibitory concentration (IC_{50}), and the inhibitory constant (K_i) values were determined using GraphPad Prism software.

In Vitro Pulldown Assay—Generation of piceatannol-Sepharose 4B was performed as described previously (23). Briefly, 0.3 g of Sepharose 4B was activated in 1 mM HCl and mixed with 2 mg piceatannol in the coupled solution of 0.1 M $NaHCO_3$ and 0.5 M NaCl. Following incubation at 4 °C overnight, the mixture was transferred to 0.1 M Tris-HCl buffer (pH 8.0) and further incubated at 4 °C overnight. The mixture was washed three times with 0.1 M acetated (pH 4.0) buffer and 0.1 M Tris buffer (pH 8.0), respectively, and suspended in PBS. *In vitro* pulldown assay was performed as described previously (27). Briefly, His-tagged active IR protein (0.2 μg) was incubated with piceatannol-Sepharose 4B or control Sepharose 4B beads. Following the incubation at 4 °C overnight, the beads were washed five times with wash buffer, and protein bound to the beads was pulled down and analyzed by immunoblotting.

ATP and Piceatannol Competition Assay—Active IR protein (0.2 μg) was incubated with 100 μl of piceatannol-Sepharose 4B or control Sepharose 4B beads in the presence or absence of 10 or 100 μM ATP in reaction buffer. After overnight incubation at 4 °C, the protein was pulled down and analyzed by immunoblotting.

Molecular Modeling—Insight II (Accelrys Inc, CA) was used for the docking study and structure analysis with the crystal coordinates of IR in complex with ATP (Protein Data Bank accession code 1IR3) and IGF-1 receptor (IGF-1R) in complex with MSC160919A (Protein Data Bank accession code 3LW0).

Statistical Analysis—Data are shown as means ± S.E. Statistical analysis was performed using SAS9.2 software. Significance of treatment effect and interactions were determined with one-way analysis of variance. Dunnett's multiple comparison analysis was used to determine the significant differences between group means. p values lower than 0.05 were regarded as statistically significant.

RESULTS

Piceatannol Inhibits Adipogenesis in 3T3-L1 Preadipocytes—We first investigated the effect of piceatannol on the differentiation of 3T3-L1 preadipocytes to adipocytes. Post-confluent 3T3-L1 preadipocytes were treated with DMI to initiate differentiation. The medium was supplemented with various concentrations of piceatannol (0–50 μM) for 6 days. Adipogenesis of these cells was assessed by Oil Red O staining of intracellular lipid droplets, CARS microscopy, and immunoblot assay of adi-

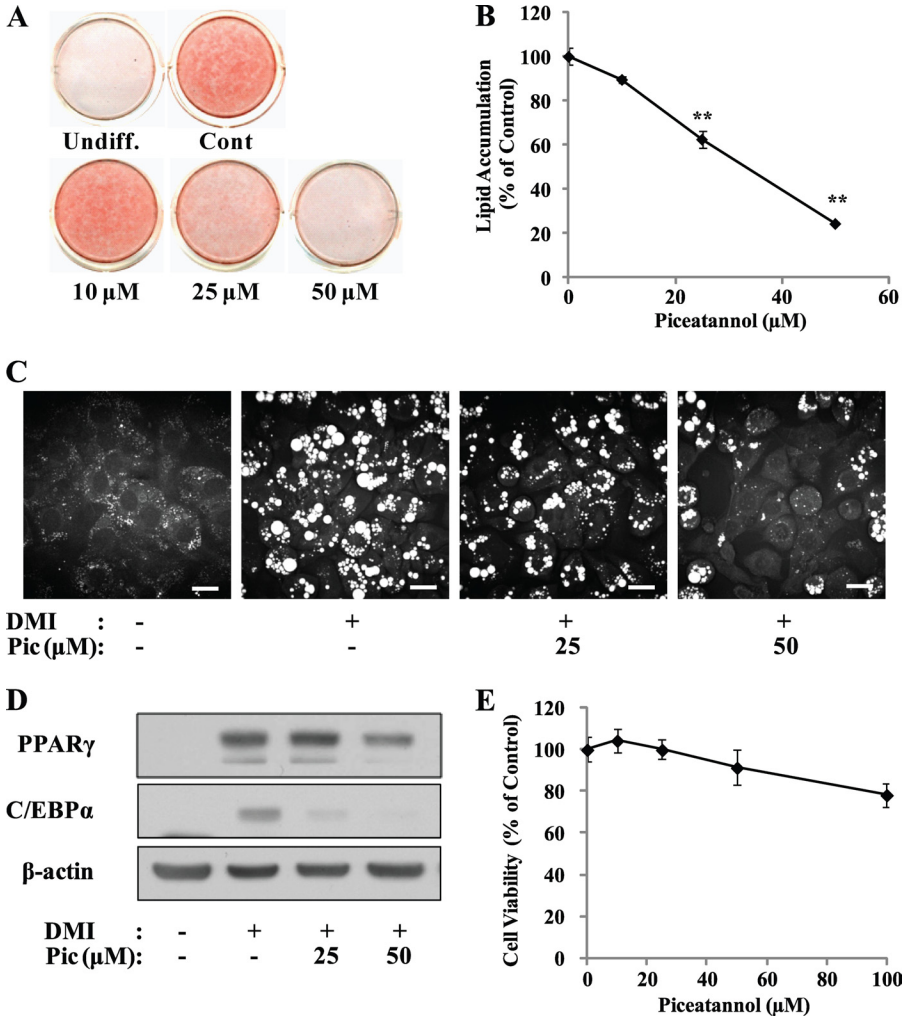

FIGURE 1. **Piceatannol inhibits adipogenesis in 3T3-L1 preadipocytes.** 3T3-L1 preadipocytes were stimulated with DMI to differentiate into mature adipocytes with or without various concentrations (0, 10, 25, and 50 μM) of piceatannol for 6 days. The undifferentiated preadipocytes (*Undiff.*), 3T3-L1 adipocytes (*Cont.*), and adipocytes differentiated with piceatannol were subjected to Oil Red O staining for visualization of lipid accumulation (*A*). *B*, Oil Red O-stained lipid droplets in these cells were extracted with isopropyl alcohol for spectrometric quantification. *C*, CARS image analysis was performed to visualize the intracellular lipid droplets in 3T3-L1 cells differentiated in the presence or absence of piceatannol (*Pic*, 25 μM and 50 μM) for 6 days. The *scale bar* indicates 20 μm. *D*, whole cell lysate was prepared from these cells to determine the expression of adipogenic marker protein PPARγ and C/EBPα by immunoblotting with their specific antibodies. β-Actin was used as a loading control. Representative images are shown. *E*, post-confluent 3T3-L1 preadipocytes were incubated with DMI and various concentrations (0–100 μM) of piceatannol for 2 days, and the viability of these cells was assessed by MTT assay. Data are presented as means ± S.E. (**, $p < 0.01$), $n = 3$, and the experiment was repeated at least twice with similar results.

pogenic transcription factors. Morphologic and quantitative analysis of intracellular lipids by Oil Red O staining showed that piceatannol-treated 3T3-L1 cells displayed a dose-dependent inhibition of adipogenesis (Fig. 1*A*). The inhibitory effect of piceatannol on adipogenesis was first noted at 25 μM, and ~80% decrease of lipid accumulation was observed at 50 μM piceatannol (Fig. 1*B*). By adopting CARS microscopy, a label-free and noninvasive microscopic imaging technique sensitive to lipid-rich molecules both *in vitro* and *in vivo* (28–30), individual lipid droplets accumulated in these cells were visually analyzed. The number and size of lipid droplets accumulated in the piceatannol-treated cells were markedly decreased compared with those in differentiated control adipocytes (Fig. 1*C*). Consistent with these results, protein levels of adipogenic transcription factors such as PPARγ and C/EBPα in 3T3-L1 cells treated with piceatannol at concentrations of 25 and 50 μM were lower than those in control cells differentiated for 6 days (Fig. 1*D*).

A recently proposed cytotoxic effect of piceatannol in other cell lines (31) prompted us to test a possibility that piceatannol-inhibited adipogenesis could result from its cytotoxic effect in 3T3-L1 cells. To test this possibility, we examined the effect of piceatannol on the viability of differentiating 3T3-L1 cells for 48 h by performing an MTT assay. Piceatannol (0–100 μM) displayed little effect on the viability of differentiating 3T3-L1 cells with a maximum 20% decrease in cell viability at 100 μM (Fig. 1*E*). Collectively, these results suggest an anti-adipogenic property of piceatannol *in vitro* without any cytotoxic effects.

Piceatannol Suppresses MCE in the Early Phase of Adipogenesis—In an effort to understand the molecular basis underlying piceatannol-inhibited adipogenesis, we first attempted to identify the key phase during the adipogenic program that is most sensitive to anti-adipogenic function of piceatannol. As Fig. 2*A* illustrates, we divided the adipogenesis process into early (days 0–2), intermediate (days 2–4), and late

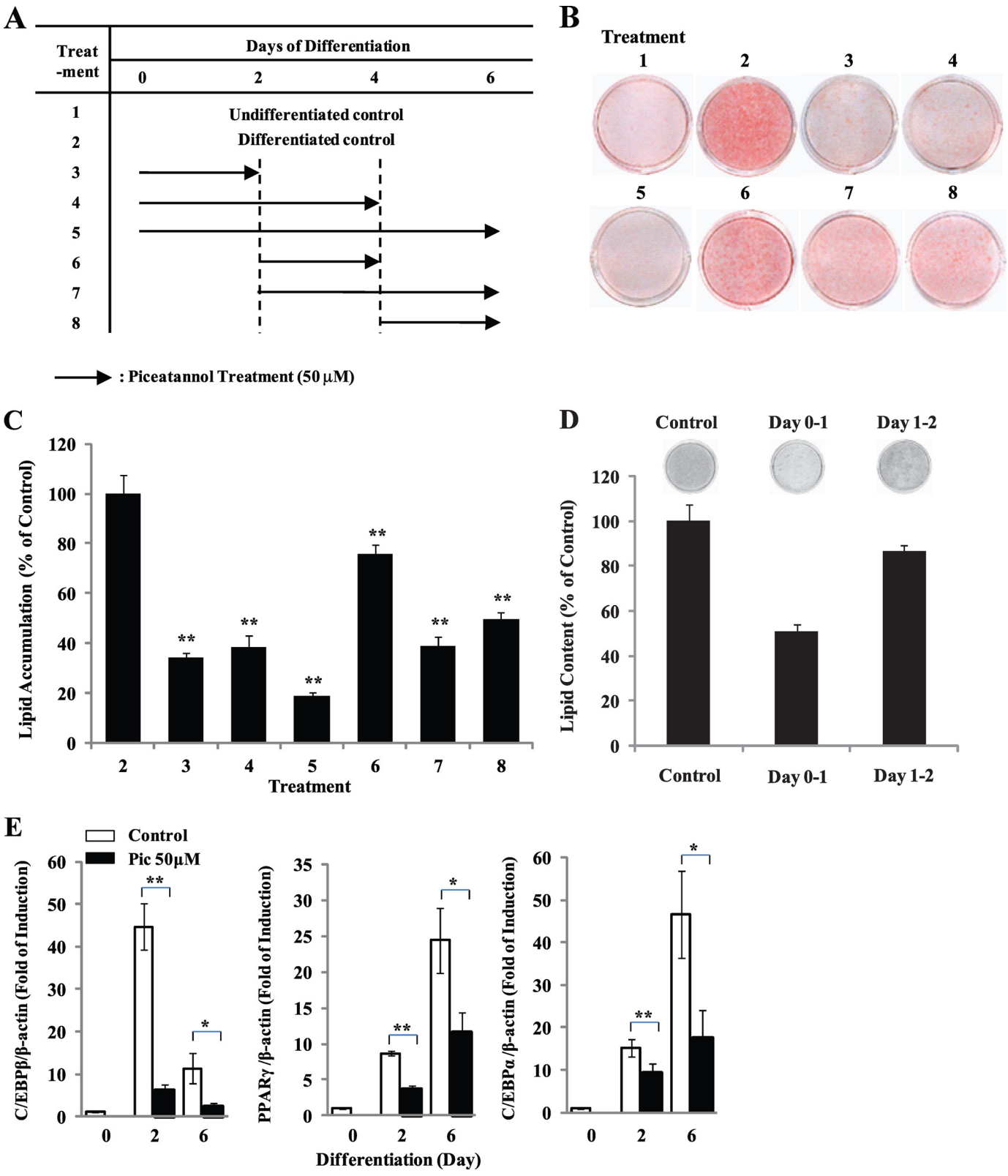

FIGURE 2. **Early stage of adipogenesis is critical for piceatannol-inhibited adipogenesis.** 3T3-L1 cells were induced with DMI to differentiate to mature adipocytes. *A*, 50 μM piceatannol was added at the indicated time (*Treatment 1–8*) during the adipogenesis. After 6 days of differentiation, these cells were subjected to Oil Red O staining for a quantitative (*B* and *D*) and qualitative (*C* and *D*) comparison of intracellular lipid accumulation. Representative images are shown. *E*, mRNA levels of PPARγ, C/EBPα, and C/EBPβ were examined in 3T3-L1 cells differentiated for 2 or 6 days in the presence or absence of 50 μM piceatannol (*Pic*) by real time PCR. The signals were normalized to β-actin, an internal control, and the data were presented as relative fold of induction. Data are presented as means ± S.E. (*, $p < 0.05$; **, $p < 0.01$), $n = 3$.

(days 4–6) phases (3). Fifty μM piceatannol was then given to the differentiating cells at the indicated times of adipogenesis. After 6 days of differentiation, these cells were subjected to a quantification of Oil Red O staining of intracellular lipids. Consistent with the result shown in Fig. 1, treatment 5 resulted in 80% inhibition of adipogenesis (Fig. 2, *B* and *C*). Moreover, the cells in treatments 3 and 4 exhibited 65–70% decrease in lipid accumulation to a similar extent as those in treatment 5. However, treatment 6 showed a 20% decrease in adipogenesis (Fig. 2*B*). In addition, the presence of piceatannol only in days 0–1 showed ~50% inhibition of adipogenesis (Fig. 2*D*). These results implicate that the inhibitory effect of piceatannol on adipogenesis is primarily attributable to its inhibitory effect during the early phase of adipogenesis. In addition, cells under the treatments 7 and 8, which included late phase (days 4–6) of adipogenesis, also displayed significantly reduced levels of lipid accumulation compared with control cells, suggesting an additional role of piceatannol in regulating the terminal adipogenesis program presumably through modulation of lipogenesis and/or fat mobilization. To further assess the effect of piceatannol on transcriptional levels of adipogenic transcription factors during adipogenesis, mRNA levels of C/EBPβ, PPARγ, and C/EBPα were measured at day 2 (the early phase) and day 6 (the late phase) of 3T3-L1 adipocytes differentiated in the presence or absence of 50 μM piceatannol. Real time PCR analysis revealed dramatically decreased mRNA levels of C/EBPβ, PPARγ, and C/EBPα in piceatannol-treated cells both at days 2 and 6 compared with nontreated control cells (Fig. 2*E*). The most striking inhibition was in the expression of C/EBPβ, an early adipogenic transcription factor linking the cell cycle progression in the MCE process and the subsequent initiation of transcription of PPARγ and C/EBPα genes in the early phase of adipogenesis. Accumulating evidence suggests a regulatory role of piceatannol in cell cycle progression in various cell types (20, 32, 33). Because induction of additional rounds of the cell cycle is a key feature of MCE progress in adipogenesis, we next examined the effect of piceatannol on cell cycle progression of 3T3-L1 preadipocytes during the MCE process. Flow cytometry assay results showed that piceatannol-treated cells displayed a delayed cell cycle progression at both 16 and 24 h after induction of differentiation with DMI (Fig. 3*A*). Approximately 50% of differentiating 3T3-L1 cells was in the S phase of the cell cycle after 16 h of DMI treatment, whereas only 15% of piceatannol-treated cells was in the S phase, and more than 80% of piceatannol-treated cells was in the G_1 phase of the cell cycle (Fig. 3*B*). This in turn resulted in 35% of DMI-treated control cells found in G_2/M phase, whereas only 10% of piceatannol-treated cells were found to be in G_2/M phase after 24 h of treatment (Fig. 3*C*). Thus, our results indicate that piceatannol impairs induction of early adipogenic transcription factors and cell cycle programs in the early phase of adipogenesis of 3T3-L1 cells.

Piceatannol Regulates Insulin Signaling Pathway in the Early Phase of Adipogenesis—An immediate induction of the insulin-signaling pathway is one of the key events in the early phase of adipogenesis, and this occurs within several hours after treatment of preadipocytes with differentiating medium containing DMI. Moreover, a recent study suggested a potential inhibitory role of piceatannol on PI3K activity in human aortic smooth muscle cells (23). Thus, we questioned whether the piceatannol effect in adipocytes involved the regulation of the insulin-signaling pathway in the early phase of adipogenesis. We first tested the effect of piceatannol on the insulin-dependent PI3K/Akt signaling pathway in the early phase of adipogenesis. Adipogenic stimuli strongly induced phosphorylation of Akt after 30 min of stimulation with a sustained level of phosphorylation up to 120 min (Fig. 4*A*). However, 50 μM piceatannol markedly inhibited DMI treatment-induced Akt phosphorylation in 3T3-L1 cells (Fig. 4*A*). Moreover, almost complete inhibition of Akt phosphorylation in DMI-treated differentiating cells was observed by treatment with 25 μM piceatannol (Fig. 4*B*). PI3K is an upstream target of insulin-induced Akt phosphorylation, and piceatannol has been reported to modulate PI3K activity through its direct binding to PI3K in human aortic smooth muscle cells (23). To investigate if piceatannol-inhibited Akt phosphorylation was due to suppression of PI3K activity and PI3K upstream regulators such as IRS-1 and IR in the early phase of adipogenesis, we next examined the effect of piceatannol on PI3K activity by performing an *in vitro* kinase assay in the presence of different concentrations of piceatannol and LY294002 (10 μM), a PI3K inhibitor. Piceatannol at both 25 and 50 μM completely inhibited PI3K kinase activity, whereas 10 μM LY294002 resulted in a moderate inhibition of PI3K activity (Fig. 4*C*). Although DMI treatment resulted in phosphorylation of both IRS-1 and IR in differentiating 3T3-L1 cells, piceatannol at 25 and 50 μM showed significant inhibition of phosphorylation of IRS-1 and IR (Fig. 4*D*). In addition, we also observed that piceatannol inhibited DMI-induced phosphorylation of ERK1/2, an extracellular serine/threonine kinase necessary for initiating adipogenesis (34, 35), in the early phase of adipogenesis but to a much lesser extent than phosphorylation of IRS-1 and IR (Fig. 4*D*). These results suggest that the piceatannol plays an inhibitory role in insulin-signaling pathway in the early phase of adipogenesis largely through modulation of insulin-induced IR-dependent phosphorylation signaling.

Piceatannol Inhibits IR Kinase Activity and Physically Interacts with IR in a Mixed Noncompetitive Manner to ATP—To elucidate whether piceatannol modulates IR function, we next examined the direct effect of various concentrations of piceatannol on IR kinase activity. Piceatannol strongly suppressed IR kinase activity in a dose-dependent manner with 75 and 100% inhibition at 50 and 100 μM, respectively (Fig. 5*A*). To further understand how piceatannol inhibits IR activity, we studied the kinetics of IR kinase. IR kinase activity followed saturation kinetics when ATP concentration was varied from 5 to 500 μM (Fig. 5*B*) with estimated K_m and V_{max} values for ATP of 57.8 μM and 1699 units/mg, respectively. We next measured IR kinase activity at each ATP concentration with respect to various piceatannol concentrations to analyze the binding kinetics of piceatannol to IR. We observed an increase in K_m values for ATP with a decrease in V_{max} at higher piceatannol concentrations (Fig. 5*C*), indicating that piceatannol exhibits mixed inhibition kinetics to IR kinase activity. Piceatannol inhibited IR kinase activity with IC_{50} values of 23–64 μM at different ATP concentrations (Fig. 5*D*). Moreover, replotting the IC_{50} values obtained from Fig. 5*C* against ATP concentrations allowed us to estimate the K_i value for piceatannol of 28.9 μM (Fig. 5*E*).

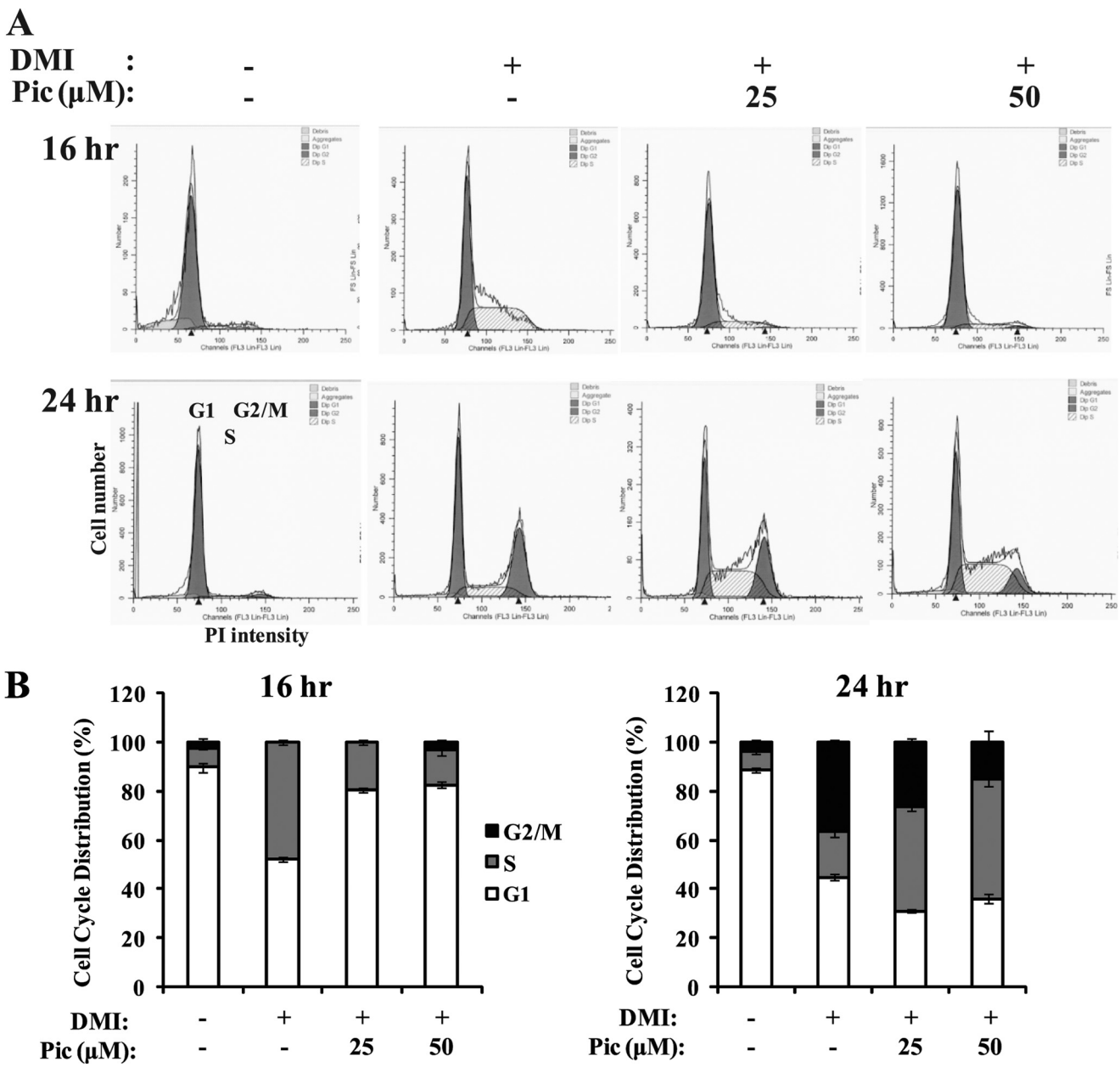

FIGURE 3. **Cell cycle analysis of 3T3-L1 cells exposed to piceatannol during MCE process of adipogenesis.** Two-day postconfluent 3T3-L1 preadipocytes were exposed to DMI in the presence or absence of 50 μM piceatannol (*Pic*) to initiate adipogenesis. The cells were harvested at 16 and 24 h after initiating differentiation and stained with propidium iodide (*PI*) for flow cytometric cell cycle analysis (*A*). The effect of piceatannol on cell cycle distribution was presented as the percent of piceatannol-treated cells in G_1, S, or G_2/M phases of cell cycle compared with nontreated control cells (*B*). The experiment was repeated at least twice with similar results.

We next examined the possibility that the inhibitory effect of piceatannol on IR kinase activity is through a physical interaction between this small molecule and an IR protein, and we conducted a pulldown assay using piceatannol-conjugated Sepharose beads. A pulldown assay using small molecule-conjugated beads has been successfully employed to various studies to elucidate direct binding between small molecules and proteins (36–38). By adopting this assay, we demonstrated that IR protein was pulled down by piceatannol-Sepharose 4B beads but not by the Sepharose 4B beads alone. The presence of His-tagged IR in the precipitated complex with piceatannol-Sepharose 4B beads was judged by immunoblot analysis using anti-His antibody (Fig. 6*A*). This result demonstrates the presence of a direct regulation of IR by piceatannol through physical interaction between the two molecules. Furthermore, the binding between piceatannol and IR was not altered by the presence of an excess amount of ATP (Fig. 6*B*). Collectively, our results suggest that piceatannol inhibits the acute activation of the insulin-signaling pathway in the early phase of adipogenesis. This is through inhibition of tyrosine kinase activity of IR via a physical interaction with this protein in a mixed noncompetitive manner to ATP.

DISCUSSION

Piceatannol is a natural polyphenolic stilbene and an analog of resveratrol. Piceatannol is synthesized in plants largely in response to environmental stress and fungal invasion. A rela-

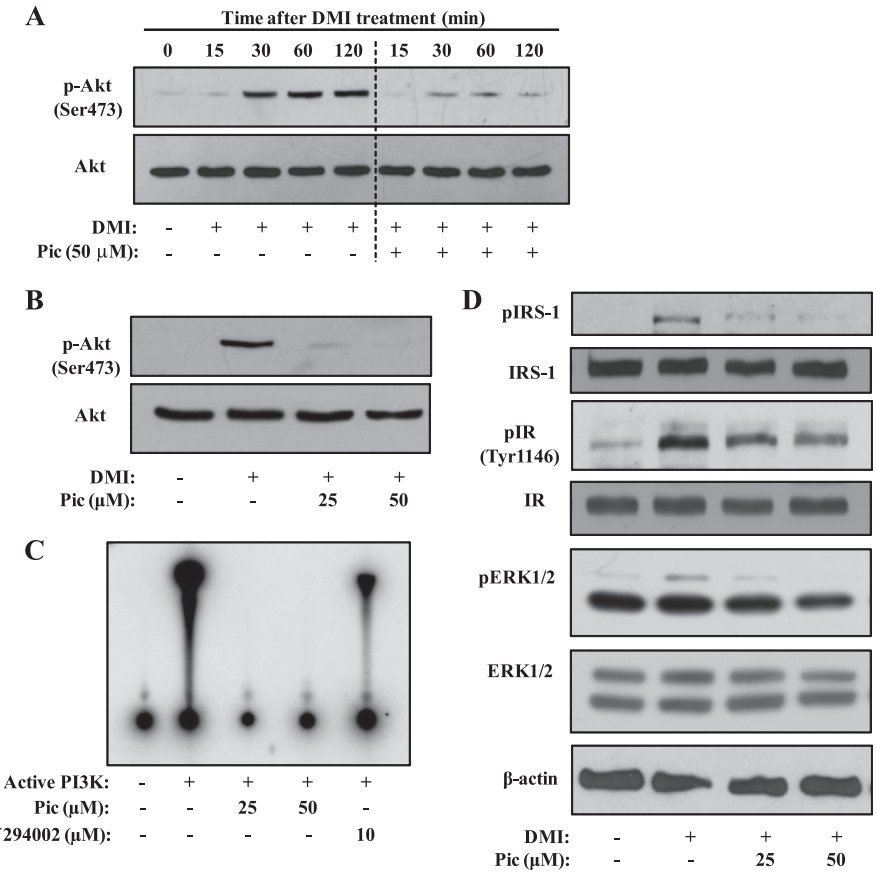

FIGURE 4. **Piceatannol inhibits DMI-induced IR/IRS-1/PI3K/Akt signaling pathway and *in vitro* PI3K activity.** *A*, 2-day postconfluent 3T3-L1 preadipocytes were stimulated with DMI in the presence or absence of piceatannol (*Pic*) for up to 2 h. Phosphorylation of Akt in differentiating cells treated with 50 μM piceatannol at the indicated time (*A*) or different concentrations of piceatannol (25 and 50 μM) for 30 min (*B*) was analyzed by immunoblot analysis as described under "Experimental Procedures" using anti-phospho-Akt (*p-Akt, Ser473*) and anti-Akt antibodies. *C*, *in vitro* kinase activity of PI3K was analyzed as described under "Experimental Procedures" in the presence or absence of piceatannol (25 and 50 μM) or 10 μM LY294002. The ^{32}P-labeled PI3-phosphate was resolved by TLC and visualized by autoradiography. *D*, phosphorylated IRS-1, IR, and ERK in 3T3-L1 cells prepared in *B* were analyzed by immunoblot analysis by anti-phosphotyrosine antibody (*pIRS-1*), anti-phospho-IRβ (*pIR, Tyr1146*) antibody, and anti-phospho-ERK antibody, respectively. β-Actin was used as a loading control. A representative image of three independent experiments is shown.

tively limited amount of piceatannol (<0.5 μg/g) rather than resveratrol has been found in fruits such as blueberry, deerberry, and grapes. However, a recent study reported that a high concentration of naturally occurring piceatannol can be seen in fruit like passion fruit (*Passiflora edulis*) (39). Up to 2.2 mg/g of piceatannol exists in freeze-dried passion fruit seed, whereas resveratrol is detected at the concentration of 0.22 mg/g. Moreover, UV irradiation has been demonstrated to produce large amounts of piceatannol in callus of peanut (40). Piceatannol is also found in resveratrol-treated cells when resveratrol is metabolized by cytochrome P450 enzyme CYP1B1 (41). Despite the well documented beneficial function of resveratrol in chemoprevention and lowering the risk of chronic diseases, including obesity (24, 25), the role of piceatannol in the aforementioned diseases has not yet been resolved.

In this study, we demonstrate that piceatannol dose-dependently inhibits adipogenesis of 3T3-L1 cells (Fig. 1). We further pinpointed that the early phase of adipogenesis, particularly in the first 24 h of adipogenesis, is largely responsible for the anti-adipogenic function of piceatannol (Fig. 2, *A–D*). The inhibitory role of piceatannol in the early phase of adipogenesis was reflected by the reduced mRNA levels of C/EBPβ, PPARγ, and C/EBPα (Fig. 2*D*). Piceatannol has been shown to inhibit cell viability and to induce apoptosis in various cell types such as macrophages (42), prostate cancer cells (43), adrenal pheochromocytoma cells (44), lymphoblasts (45), and neutrophils (46). However, our result showed that the viability of the differentiating 3T3-L1 cells was not significantly influenced by piceatannol treatment up to concentration of 100 μM (Fig. 1*E*). This result allowed us to eliminate the possibility that piceatannol-induced cellular cytotoxicity is responsible for its inhibition of adipogenesis. The pro-apoptotic property of piceatannol in other cell types has been shown to be correlated with an induction of cell cycle arrest at the G_2/M phase (18). Indeed, our cell cycle analysis result mirrors this phenomenon with delayed cell cycle progression of differentiating 3T3-L1 cells by piceatannol treatment after 24 h of DMI treatment. During the first 24 h of adipogenesis, transient activation of insulin- and IGF-1-signaling pathways coincides with expression of C/EBPβ protein and its phosphorylational activation, which are thought to be important for further induction of adipogenic transcriptional events (11, 12). Within several hours of insulin treatment in differentiating 3T3-L1 preadipocytes, an immediate stimulation of IR phosphorylation and its subsequent activation of the PI3K/Akt-signaling pathway were observed in differentiating 3T3-L1 cells (7, 47). Insulin-activated MAPK and glycogen syn-

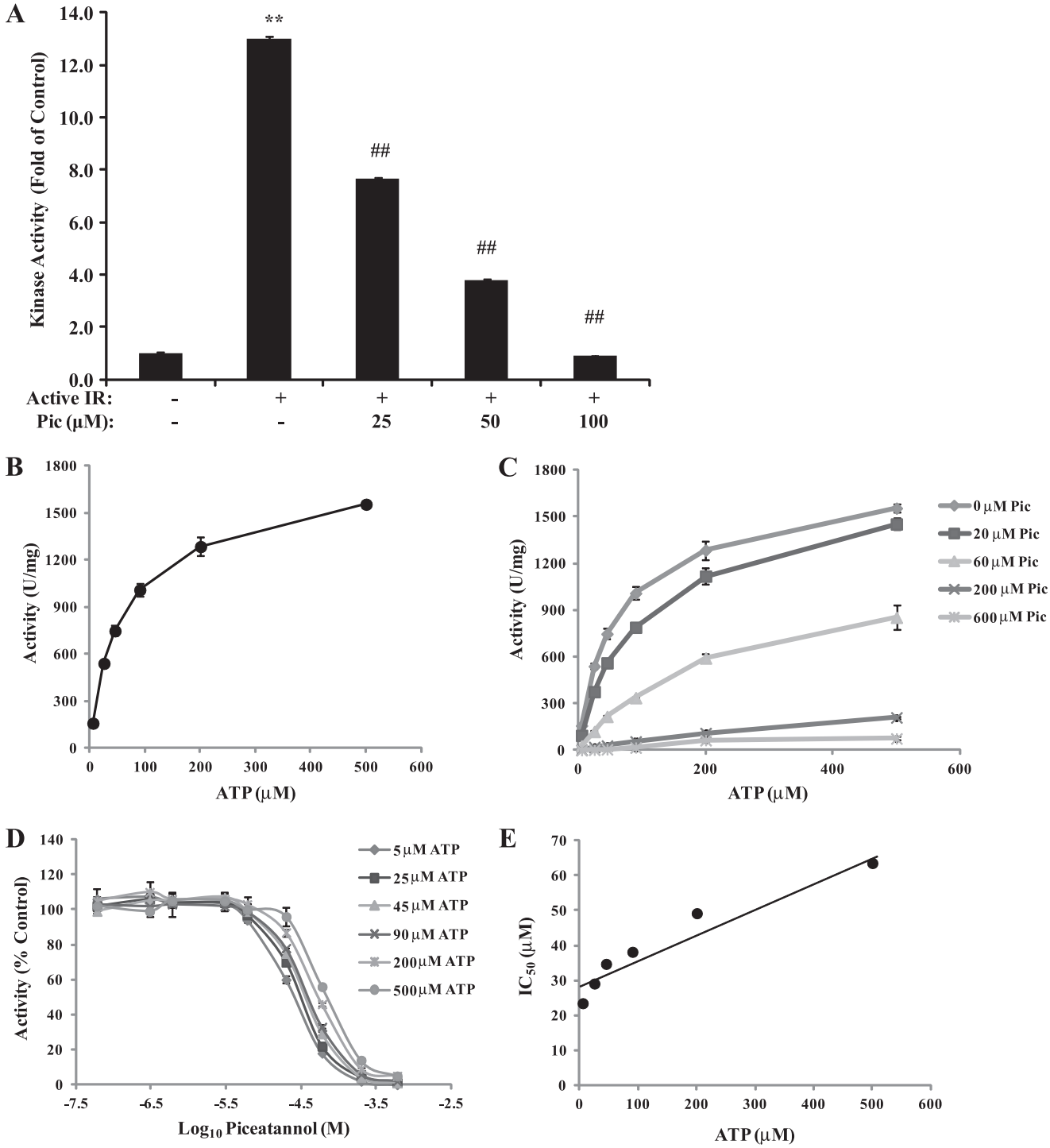

FIGURE 5. **Effect of piceatannol on the kinetics of IR kinase.** *A*, *in vitro* kinase activity of IR was measured in the presence or absence of various concentrations of piceatannol (*Pic*). His-IR protein (50 ng) was incubated with piceatannol (25, 50, or 100 μM) at 30 °C for 10 min followed by additional 10-min incubation with IRS-1 derived peptide and [γ-^{32}P]ATP. The radioactive incorporation onto IRS-1 was determined using a scintillation counter. (**, $p < 0.01$, compared with control; ##, $p < 0.01$, compared with IR active). *B*, IR kinase activity was measured as a function of the concentration of ATP at 5, 25, 45, 90, 200, and 500 μM. The Michaelis-Menten constant (K_m) and maximum activity (V_{max}) were determined as described under "Experimental Procedures." *C* and *D*, IR kinase activity was measured as a function of the concentration of ATP (5–500 μM) in the presence of various concentrations of piceatannol (0–600 μM). *E*, IC_{50} values calculated from *D* was replotted against ATP concentration to determine the K_i value of piceatannol. The *y*-intercept of the slope in this graph represents K_i value of piceatannol.

thase kinase 3β during this time are further known to promote phosphorylation of C/EBPβ and its transcriptional activity within 16 h of induction of adipogenesis (11, 12). Because the critical role of IR in adipose development has been demonstrated in IR-deficient mice (15), it would be reasonable to assume that transient control of IR activity in the early phase of adipogenesis could impact adipocyte differentiation. We then investigated the effect of piceatannol on the IR-dependent PI3K/Akt pathway in the early phase of adipogenesis. Our series of immunoblot analyses showed that piceatannol inhibited

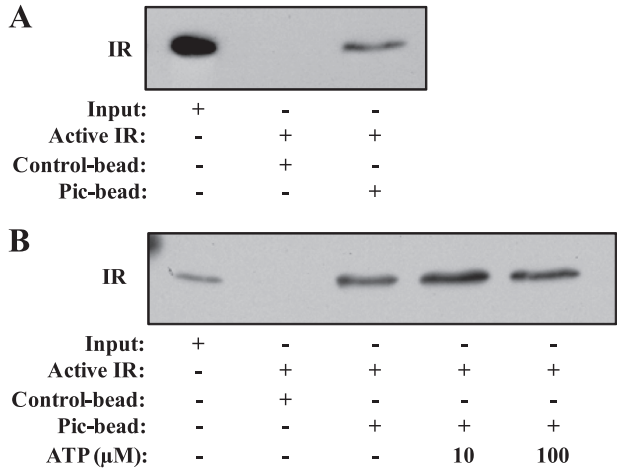

FIGURE 6. **Piceatannol directly binds to IR.** *A,* His-IR protein was incubated with control-Sepharose 4B or Sepharose 4B conjugated with piceatannol (*Pic*) at 4 °C overnight. IR-piceatannol-Sepharose 4B complex was pulled down by centrifugation, and the precipitated IR was analyzed by immunoblot analysis using anti-His antibody. *B,* IR protein was incubated with control-Sepharose 4B or piceatannol-Sepharose 4B in the presence of indicated concentrations of ATP at 4 °C overnight. The IR bound to the piceatannol-Sepharose 4B beads was pulled down by centrifugation and analyzed by immunoblot analysis using anti-His antibody.

insulin-stimulated phosphorylation of IR, IRS-1, and Akt. It should be noted that a substantial inhibition of insulin-induced Akt phosphorylation and PI3K activity was observed when differentiating preadipocytes were exposed to even low concentrations of piceatannol (*e.g.* 25 μM) (Fig. 4, *B* and *C*). However, 25 μM piceatannol inhibited ~50% of lipid accumulation (Fig. 2*D*) and IR kinase activity (Fig. 5, *A* and *C*). In addition, we also observed that piceatannol inhibited DMI-induced phosphorylation of ERK1/2, which is necessary for initiating the early phase of adipogenesis, but to a much lesser extent than phosphorylation of IR, IRS-1, and Akt (Fig. 4*D*). Although the significance of our study is to identify IR as a novel target for the anti-adipogenic function of piceatannol, it would be possible that the piceatannol-inhibited insulin-signaling pathway in the early phase of adipogenesis is a combined result from the direct inhibitory effect of piceatannol on IR as well as PI3K activities. Supporting this notion, a low concentration of piceatannol (0–20 μM) is able to effectively inhibit Akt phosphorylation and PI3K activity in platelet-derived growth factor-treated human aortic smooth muscle cells. Furthermore, a study of physical binding between piceatannol and PI3K by which piceatannol inhibits PI3K activity has been reported (23). Although piceatannol is suggested to be poorly absorbed in cells, we observed intracellular piceatannol absorbed in 3T3-L1 preadipocytes after 24 h of treatment (data not shown). Thus, we speculate that the piceatannol-inhibited insulin-signaling pathway in differentiating 3T3-L1 cells is a combined result from a direct binding of piceatannol to IR on the cell surface and possibly to intracellular PI3K in preadipocytes, which in turn results in effective suppression of Akt phosphorylation by piceatannol even at lower concentrations. More studies are needed to determine how intracellular piceatannol modulates the insulin-signaling pathway in the early phase of adipogenesis.

To have insights into the IR inhibition mechanism by piceatannol, we carried out kinetics and modeling studies of interaction between piceatannol and IR. The K_m value of IR for ATP is 57.8 μM, and this is in agreement with a previously reported K_m value of 58 μM for ATP of IR kinase in rat adipocytes (48). Our data clearly demonstrate that piceatannol is a mixed noncompetitive inhibitor to ATP, by which it results in a marked increase in K_m values and a decrease in the V_{max} value of IR in relation to increasing concentrations of piceatannol. This result indicates that piceatannol and ATP could interact with IR at different binding sites. Recently, it was reported that the compounds of the indole alkylamine scaffold bind to IGF-1R, sharing a high sequence identity of 84% in the tyrosine kinase domain with IR, in an ATP-noncompetitive manner (49). Based on this finding, we simulated whether piceatannol could be docked to the pocket separate from the ATP-binding site of the kinase domain of IR crystal structure in its inactive conformation (49, 50). Fig. 7*A* shows that piceatannol and ATP-binding sites in IR are likely to be separate but adjacent to each other. The predicted binding mode of piceatannol is somewhat similar to that of MSC160910A (49). The hydroxyl group of piceatannol at the 4′ position can make a hydrogen bond with the backbone carbonyl group of Val-1060 and the hydroxyl groups at the 3 and 5 positions interact with the side chains of Glu-1047 and Asp-1132 via hydrogen bonds. In addition, several van der Waals interactions exist with the hydrophobic surface formed by Met-1051, Phe-1054, Met-1076, His-1130, and Phe-1128 (Fig. 7*A*). The putative piceatannol-binding site partially overlaps the activation loop site of the kinase domain of IR in the active conformation (Fig. 7*B*). Collectively, these results elucidate IR as an important target for the anti-adipogenic property of piceatannol. It should be also noted that our study also provides evidence of a potential inhibitory role of piceatannol in the late phase of adipogenesis (Fig. 2*C*). The presence of piceatannol from days 4 to 6 of adipogenesis resulted in a significant suppression of lipid droplet accumulation in 3T3-L1 cells. Presumably, its inhibitory role in the late phase of adipogenesis is likely to be due to modulation of either lipogenesis or lipolysis. Although little is known about the role of piceatannol in lipid metabolism, resveratrol has been shown to inhibit total fatty acid and triglyceride synthesis in adipocytes (51, 52). Current evidence also suggests a role for resveratrol in stimulating lipolysis and fatty acid oxidation in adipocytes (53–55). Thus, it will be of interest to determine the role of piceatannol in lipid synthesis and hydrolysis in adipose tissue.

Piceatannol is best known as a potent inhibitor of Syk. Syk is a 72-kDa nonreceptor tyrosine kinase with an N-terminal tandem pair of Src homology 2 domains and a C-terminal catalytic domain, which mediates immunoreceptor signaling events involved in proliferation, differentiation, and phagocytosis of hematopoietic cells (56). It is also reported to suppress interferon α-induced tyrosine phosphorylation of signal transducers and activator of transcription (STAT)3 and STAT5 (57), and other serine/threonine protein kinases such as cyclic AMP-dependent protein kinase, phospholipid-dependent protein kinase C, and Ca^{2+}-calmodulin-dependent myosin light chain kinase (58). Interestingly, tyrosine-phosphorylated Syk was found in the early phase of adipogenesis with its maximum level at 18–24 h after induction of differentiation with dexamethasone and 3-isobutyl-1-methylxanthine in the absence of insulin

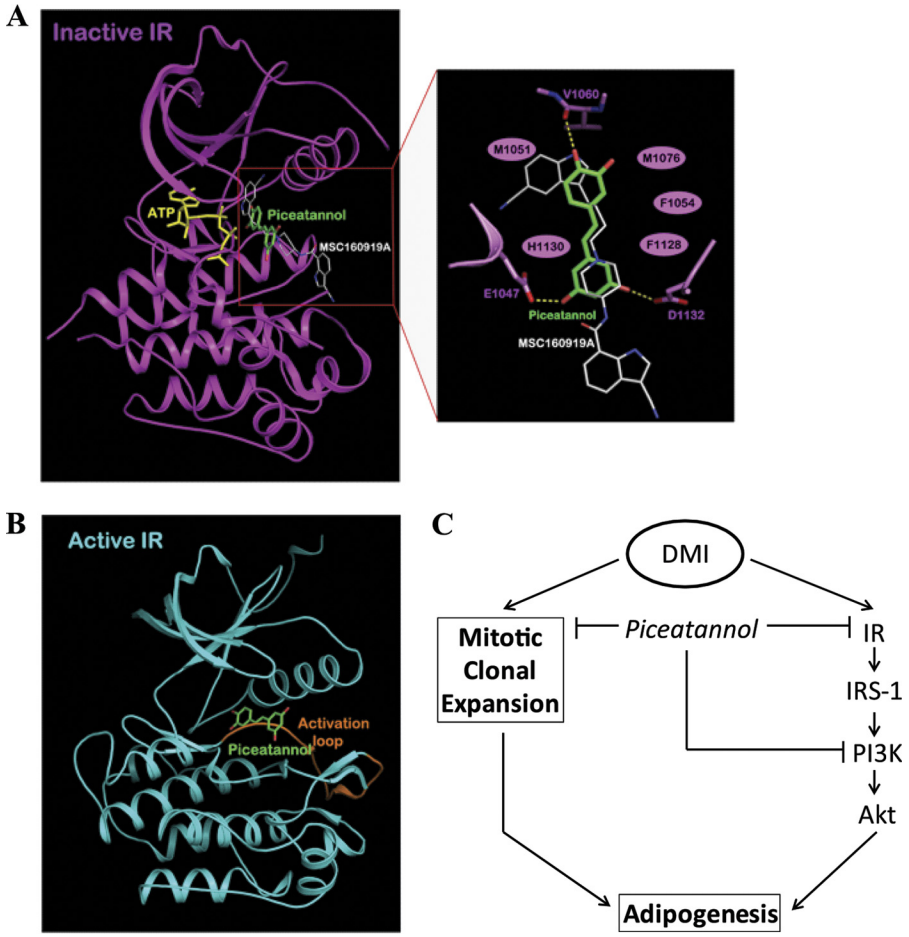

FIGURE 7. **Modeling study of piceatannol binding to IR.** *A*, hypothetical model of IR-piceatannol complex with its close-up view. Piceatannol (atomic color with *green* carbons) binds to the pocket adjacent to the ATP (*yellow*)-binding site of IR in the inactive conformation. MSC160919A (atomic color with *white* carbons) is overlaid on the model structure of the complex for comparison. The residues involved in the interactions with piceatannol are indicated. The hydrogen bonds are depicted as *dashed lines* and the van der Waals interactions as *ellipses*. *B*, activation loop of the active IR. The activation loop in the active conformation is colored in *orange*. Piceatannol (atomic color with *green* carbons) is overlaid on the active structure for comparison. *C*, speculated model for how piceatannol regulates adipogenesis of 3T3-L1 preadipocytes. Piceatannol inhibits DMI-induced early cellular processes during adipogenesis. Piceatannol attenuates mitotic clonal expansion of differentiating cells by delaying the cell cycle progression. Parallel to this, piceatannol suppresses IR-dependent signaling pathway in the early phase of adipogenesis by a direct interaction with IR and inhibition of its kinase activity. Simultaneously, piceatannol also inhibits PI3K activity. Collectively, these result in suppression of Akt phosphorylation and adipogenesis.

in 3T3-L1 cells (59). Moreover, ectopic expression of Syk resulted in enhanced adipogenesis *in vitro* (59). Given the role of piceatannol in inhibiting diverse target kinase activities, including Syk, it will be of interest to study the requirement of Syk for adipogenesis and the role of piceatannol in Syk function in the early phase of adipogenesis.

Although many dietary small molecules are proposed to have health benefits, poor bioavailability with low solubility in the aqueous system generally limits the efficacy of these in physiological conditions. For instance, a single intravenous dose of 10 mg/kg piceatannol in rats resulted in a decline of plasma piceatannol concentrations from ~41 to 1 μM in 6 h (60). Similarly, a single i.v. administration of resveratrol (20 mg/kg) to rats showed maximum plasma concentrations of resveratrol and its metabolites in the range from 2 to 13 μM (61). However, a number of studies demonstrated that the poor bioavailability of resveratrol can be enhanced by various methods such as encapsulation with cyclodextrin, formulation with piperine, and incorporation of resveratrol into microparticles, liposomes, nanocapsules, and emulsion (62). For example, oral administration of a single high dose of resveratrol (100 mg/kg) in mice with or without piperine (10 mg/kg) supplementation resulted in a dramatic increase in maximum plasma resveratrol concentration from 10 to 154 μM (63). Furthermore, a repeated dose of resveratrol up to 5 g/day, which is equivalent to ~85 mg/kg for a 60-kg man, has been shown to be safe in humans (64). Because piceatannol is often compared with resveratrol due to their similar chemical structures, these studies underscore the importance of the development of a novel piceatannol formulation that would allow us to overcome its poor solubility and bioavailability *in vivo*, thereby achieving elevated plasma concentration of piceatannol for exerting its maximum health benefit. However, piceatannol was reported to inhibit its target kinases at K_i values of 3–20 μM (58, 65, 66). In line with this, our finding of a 50% inhibition of adipogenesis at ~30 μM piceatannol and a K_i value of piceatannol for IR activity at 28.9 μM *in vitro* indicates that these concentrations are possibly achievable in a physiological condition when piceatannol is administrated with improved formulation and/or structural modification.

In summary, our study suggests a new role of piceatannol in adipogenesis through targeting the early biochemical and cellular events of adipogenesis such as insulin-dependent signaling pathway, MCE, and expression of early adipogenic transcription factors (a suggested mechanism of piceatannol-inhibited adipogenesis is summarized as a schematic in Fig. 7*C*). Although we cannot rule out the possibility that piceatannol has additional effects on adipogenesis, our finding of a direct binding between piceatannol and IR and the inhibitory role of piceatannol in IR tyrosine kinase activity and its subsequent phosphorylation cascade of insulin-signaling pathway reveals a new mechanism by which a natural polyphenolic stilbene modulates adipogenesis.

Acknowledgments—We thank Dr. Kola Ajuwon and the members of the Kim Laboratory the for careful review and helpful editing of the manuscript.

REFERENCES

1. Kopelman, P. G. (2000) Obesity as a medical problem. *Nature* **404,** 635–643
2. Spalding, K. L., Arner, E., Westermark, P. O., Bernard, S., Buchholz, B. A., Bergmann, O., Blomqvist, L., Hoffstedt, J., Näslund, E., Britton, T., Concha, H., Hassan, M., Rydén, M., Frisén, J., and Arner, P. (2008) Dynamics of fat cell turnover in humans. *Nature* **453,** 783–787
3. Gregoire, F. M., Smas, C. M., and Sul, H. S. (1998) Understanding adipocyte differentiation. *Physiol. Rev.* **78,** 783–809
4. Rosen, E. D., and MacDougald, O. A. (2006) Adipocyte differentiation from the inside out. *Nat. Rev. Mol. Cell Biol.* **7,** 885–896
5. Farmer, S. R. (2006) Transcriptional control of adipocyte formation. *Cell Metab.* **4,** 263–273
6. Gagnon, A., Chen, C. S., and Sorisky, A. (1999) Activation of protein kinase B and induction of adipogenesis by insulin in 3T3-L1 preadipocytes. Contribution of phosphoinositide-3,4,5-trisphosphate *versus* phosphoinositide 3,4-bisphosphate. *Diabetes* **48,** 691–698
7. Sakaue, H., Ogawa, W., Matsumoto, M., Kuroda, S., Takata, M., Sugimoto, T., Spiegelman, B. M., and Kasuga, M. (1998) Post-transcriptional control of adipocyte differentiation through activation of phosphoinositide 3-kinase. *J. Biol. Chem.* **273,** 28945–28952
8. Kim, S. W., Muise, A. M., Lyons, P. J., and Ro, H. S. (2001) Regulation of adipogenesis by a transcriptional repressor that modulates MAPK activation. *J. Biol. Chem.* **276,** 10199–10206
9. Tang, Q. Q., Otto, T. C., and Lane, M. D. (2003) Mitotic clonal expansion. A synchronous process required for adipogenesis. *Proc. Natl. Acad. Sci. U.S.A.* **100,** 44–49
10. Prusty, D., Park, B. H., Davis, K. E., and Farmer, S. R. (2002) Activation of MEK/ERK signaling promotes adipogenesis by enhancing peroxisome proliferator-activated receptor γ (PPARγ) and C/EBPα gene expression during the differentiation of 3T3-L1 preadipocytes. *J. Biol. Chem.* **277,** 46226–46232
11. Tang, Q. Q., Grønborg, M., Huang, H., Kim, J. W., Otto, T. C., Pandey, A., and Lane, M. D. (2005) Sequential phosphorylation of CCAAT enhancer-binding protein β by MAPK and glycogen synthase kinase 3β is required for adipogenesis. *Proc. Natl. Acad. Sci. U.S.A.* **102,** 9766–9771
12. Tang, Q. Q., and Lane, M. D. (1999) Activation and centromeric localization of CCAAT/enhancer-binding proteins during the mitotic clonal expansion of adipocyte differentiation. *Genes Dev.* **13,** 2231–2241
13. Tang, Q. Q., Otto, T. C., and Lane, M. D. (2003) CCAAT/enhancer-binding protein β is required for mitotic clonal expansion during adipogenesis. *Proc. Natl. Acad. Sci. U.S.A.* **100,** 850–855
14. Blüher, M., Michael, M. D., Peroni, O. D., Ueki, K., Carter, N., Kahn, B. B., and Kahn, C. R. (2002) Adipose tissue selective insulin receptor knockout protects against obesity and obesity-related glucose intolerance. *Dev. Cell* **3,** 25–38
15. Blüher, M., Patti, M. E., Gesta, S., Kahn, B. B., and Kahn, C. R. (2004) Intrinsic heterogeneity in adipose tissue of fat-specific insulin receptor knock-out mice is associated with differences in patterns of gene expression. *J. Biol. Chem.* **279,** 31891–31901
16. Valverde, A. M., Kahn, C. R., and Benito, M. (1999) Insulin signaling in insulin receptor substrate (IRS)-1-deficient brown adipocytes. Requirement of IRS-1 for lipid synthesis. *Diabetes* **48,** 2122–2131
17. Garofalo, R. S., Orena, S. J., Rafidi, K., Torchia, A. J., Stock, J. L., Hildebrandt, A. L., Coskran, T., Black, S. C., Brees, D. J., Wicks, J. R., McNeish, J. D., and Coleman, K. G. (2003) Severe diabetes, age-dependent loss of adipose tissue, and mild growth deficiency in mice lacking Akt2/PKBβ. *J. Clin. Invest.* **112,** 197–208
18. Larrosa, M., Tomás-Barberán, F. A., and Espín, J. C. (2004) The grape and wine polyphenol piceatannol is a potent inducer of apoptosis in human SK-Mel-28 melanoma cells. *Eur. J. Nutr.* **43,** 275–284
19. Ferrigni, N. R., McLaughlin, J. L., Powell, R. G., and Smith, C. R., Jr. (1984) Use of potato disc and brine shrimp bioassays to detect activity and isolate piceatannol as the antileukemic principle from the seeds of *Euphorbia lagascae*. *J. Nat. Prod.* **47,** 347–352
20. Wolter, F., Clausnitzer, A., Akoglu, B., and Stein, J. (2002) Piceatannol, a natural analog of resveratrol, inhibits progression through the S phase of the cell cycle in colorectal cancer cell lines. *J. Nutr.* **132,** 298–302
21. Son, P. S., Park, S. A., Na, H. K., Jue, D. M., Kim, S., and Surh, Y. J. (2010) Piceatannol, a catechol-type polyphenol, inhibits phorbol ester-induced NF-κB activation and cyclooxygenase-2 expression in human breast epithelial cells. Cysteine 179 of IKKβ as a potential target. *Carcinogenesis* **31,** 1442–1449
22. Ashikawa, K., Majumdar, S., Banerjee, S., Bharti, A. C., Shishodia, S., and Aggarwal, B. B. (2002) Piceatannol inhibits TNF-induced NF-κB activation and NF-κB-mediated gene expression through suppression of IκBα kinase and p65 phosphorylation. *J. Immunol.* **169,** 6490–6497
23. Choi, K. H., Kim, J. E., Song, N. R., Son, J. E., Hwang, M. K., Byun, S., Kim, J. H., Lee, K. W., and Lee, H. J. (2010) Phosphoinositide 3-kinase is a novel target of piceatannol for inhibiting PDGF-BB-induced proliferation and migration in human aortic smooth muscle cells. *Cardiovasc. Res.* **85,** 836–844
24. Lagouge, M., Argmann, C., Gerhart-Hines, Z., Meziane, H., Lerin, C., Daussin, F., Messadeq, N., Milne, J., Lambert, P., Elliott, P., Geny, B., Laakso, M., Puigserver, P., and Auwerx, J. (2006) Resveratrol improves mitochondrial function and protects against metabolic disease by activating SIRT1 and PGC-1α. *Cell* **127,** 1109–1122
25. Baur, J. A., Pearson, K. J., Price, N. L., Jamieson, H. A., Lerin, C., Kalra, A., Prabhu, V. V., Allard, J. S., Lopez-Lluch, G., Lewis, K., Pistell, P. J., Poosala, S., Becker, K. G., Boss, O., Gwinn, D., Wang, M., Ramaswamy, S., Fishbein, K. W., Spencer, R. G., Lakatta, E. G., Le Couteur, D., Shaw, R. J., Navas, P., Puigserver, P., Ingram, D. K., de Cabo, R., and Sinclair, D. A. (2006) Resveratrol improves health and survival of mice on a high calorie diet. *Nature* **444,** 337–342
26. Le, T. T., Langohr, I. M., Locker, M. J., Sturek, M., and Cheng, J. X. (2007) Label-free molecular imaging of atherosclerotic lesions using multimodal nonlinear optical microscopy. *J. Biomed. Opt.* **12,** 054007
27. Lee, K. W., Kang, N. J., Heo, Y. S., Rogozin, E. A., Pugliese, A., Hwang, M. K., Bowden, G. T., Bode, A. M., Lee, H. J., and Dong, Z. (2008) Raf and MEK protein kinases are direct molecular targets for the chemopreventive effect of quercetin, a major flavonol in red wine. *Cancer Res.* **68,** 946–955
28. Evans, C. L., and Xie, X. S. (2008) Coherent anti-Stokes Raman scattering microscopy. Chemical imaging for biology and medicine. *Annu. Rev. Anal. Chem.* **1,** 883–909
29. Wang, H. W., Fu, Y., Huff, T. B., Le, T. T., Wang, H., and Cheng, J. X. (2009) Chasing lipids in health and diseases by coherent anti-Stokes Raman scattering microscopy. *Vib. Spectrosc.* **50,** 160–167
30. Kim, C. Y., Bordenave, N., Ferruzzi, M. G., Safavy, A., and Kim, K. H. (2011) Modification of curcumin with polyethylene glycol enhances the delivery of curcumin in preadipocytes and its antiadipogenic property. *J. Agric. Food Chem.* **59,** 1012–1019
31. Chowdhury, S. A., Kishino, K., Satoh, R., Hashimoto, K., Kikuchi, H., Nishikawa, H., Shirataki, Y., and Sakagami, H. (2005) Tumor specificity and apoptosis inducing activity of stilbenes and flavonoids. *Anticancer Res.* **25,**

2055–2063
32. Lee, B., Lee, E. J., Kim, D. I., Park, S. K., Kim, W. J., and Moon, S. K. (2009) Inhibition of proliferation and migration by piceatannol in vascular smooth muscle cells. *Toxicol. In Vitro* **23,** 1284–1291
33. Lee, Y. M., Lim do, Y., Cho, H. J., Seon, M. R., Kim, J. K., Lee, B. Y., and Park, J. H. (2009) Piceatannol, a natural stilbene from grapes, induces G_1 cell cycle arrest in androgen-insensitive DU145 human prostate cancer cells via the inhibition of CDK activity. *Cancer Lett.* **285,** 166–173
34. Bost, F., Aouadi, M., Caron, L., and Binétruy, B. (2005) The role of MAPKs in adipocyte differentiation and obesity. *Biochimie* **87,** 51–56
35. Bost, F., Aouadi, M., Caron, L., Even, P., Belmonte, N., Prot, M., Dani, C., Hofman, P., Pagès, G., Pouysségur, J., Le Marchand-Brustel, Y., and Binétruy, B. (2005) The extracellular signal-regulated kinase isoform ERK1 is specifically required for *in vitro* and *in vivo* adipogenesis. *Diabetes* **54,** 402–411
36. Lee, D. E., Lee, K. W., Jung, S. K., Lee, E. J., Hwang, J. A., Lim, T. G., Kim, B. Y., Bode, A. M., Lee, H. J., and Dong, Z. (2011) 6,7,4′-Trihydroxyisoflavone inhibits HCT-116 human colon cancer cell proliferation by targeting CDK1 and CDK2. *Carcinogenesis* **32,** 629–635
37. Lee, D. E., Lee, K. W., Song, N. R., Seo, S. K., Heo, Y. S., Kang, N. J., Bode, A. M., Lee, H. J., and Dong, Z. (2010) 7,3′,4′-Trihydroxyisoflavone inhibits epidermal growth factor-induced proliferation and transformation of JB6 P^+ mouse epidermal cells by suppressing cyclin-dependent kinases and phosphatidylinositol 3-kinase. *J. Biol. Chem.* **285,** 21458–21466
38. Kwon, J. Y., Lee, K. W., Kim, J. E., Jung, S. K., Kang, N. J., Hwang, M. K., Heo, Y. S., Bode, A. M., Dong, Z., and Lee, H. J. (2009) Delphinidin suppresses ultraviolet B-induced cyclooxygenases-2 expression through inhibition of MAPKK4 and PI 3-kinase. *Carcinogenesis* **30,** 1932–1940
39. Matsui, Y., Sugiyama, K., Kamei, M., Takahashi, T., Suzuki, T., Katagata, Y., and Ito, T. (2010) Extract of passion fruit (*Passiflora edulis*) seed containing high amounts of piceatannol inhibits melanogenesis and promotes collagen synthesis. *J. Agric. Food Chem.* **58,** 11112–11118
40. Ku, K. L., Chang, P. S., Cheng, Y. C., and Lien, C. Y. (2005) Production of stilbenoids from the callus of *Arachis hypogaea*. A novel source of the anticancer compound piceatannol. *J. Agric. Food Chem.* **53,** 3877–3881
41. Potter, G. A., Patterson, L. H., Wanogho, E., Perry, P. J., Butler, P. C., Ijaz, T., Ruparelia, K. C., Lamb, J. H., Farmer, P. B., Stanley, L. A., and Burke, M. D. (2002) The cancer preventative agent resveratrol is converted to the anticancer agent piceatannol by the cytochrome P450 enzyme CYP1B1. *Br. J. Cancer* **86,** 774–778
42. Kang, C. H., Moon, D. O., Choi, Y. H., Choi, I. W., Moon, S. K., Kim, W. J., and Kim, G. Y. (2011) Piceatannol enhances TRAIL-induced apoptosis in human leukemia THP-1 cells through Sp1- and ERK-dependent DR5 up-regulation. *Toxicol. In Vitro* **25,** 605–612
43. Kim, E. J., Park, H., Park, S. Y., Jun, J. G., and Park, J. H. (2009) The grape component piceatannol induces apoptosis in DU145 human prostate cancer cells via the activation of extrinsic and intrinsic pathways. *J. Med. Food* **12,** 943–951
44. Jang, Y. J., Kim, J. E., Kang, N. J., Lee, K. W., and Lee, H. J. (2009) Piceatannol attenuates 4-hydroxynonenal-induced apoptosis of PC12 cells by blocking activation of c-Jun N-terminal kinase. *Ann. N.Y. Acad. Sci.* **1171,** 176–182
45. Wieder, T., Prokop, A., Bagci, B., Essmann, F., Bernicke, D., Schulze-Osthoff, K., Dörken, B., Schmalz, H. G., Daniel, P. T., and Henze, G. (2001) Piceatannol, a hydroxylated analog of the chemopreventive agent resveratrol, is a potent inducer of apoptosis in the lymphoma cell line BJAB and in primary leukemic lymphoblasts. *Leukemia* **15,** 1735–1742
46. Avdi, N. J., Nick, J. A., Whitlock, B. B., Billstrom, M. A., Henson, P. M., Johnson, G. L., and Worthen, G. S. (2001) Tumor necrosis factor-α activation of the c-Jun N-terminal kinase pathway in human neutrophils. Integrin involvement in a pathway leading from cytoplasmic tyrosine kinases apoptosis. *J. Biol. Chem.* **276,** 2189–2199
47. Xu, J., and Liao, K. (2004) Protein kinase B/AKT 1 plays a pivotal role in insulin-like growth factor-1 receptor signaling induced 3T3-L1 adipocyte differentiation. *J. Biol. Chem.* **279,** 35914–35922
48. Häring, H., Kirsch, D., Obermaier, B., Ermel, B., and Machicao, F. (1986) Tumor-promoting phorbol esters increase the Km of the ATP-binding site of the insulin receptor kinase from rat adipocytes. *J. Biol. Chem.* **261,** 3869–3875
49. Heinrich, T., Grädler, U., Böttcher, H., Blaukat, A., and Shutes, A. (2010) Allosteric IGF-1R inhibitors. *ACS Med. Chem. Lett.* **1,** 199–203
50. Hubbard, S. R. (1997) Crystal structure of the activated insulin receptor tyrosine kinase in complex with peptide substrate and ATP analog. *EMBO J.* **16,** 5572–5581
51. Pandey, P. R., Okuda, H., Watabe, M., Pai, S. K., Liu, W., Kobayashi, A., Xing, F., Fukuda, K., Hirota, S., Sugai, T., Wakabayashi, G., Koeda, K., Kashiwaba, M., Suzuki, K., Chiba, T., Endo, M., Fujioka, T., Tanji, S., Mo, Y. Y., Cao, D., Wilber, A. C., and Watabe, K. (2011) Resveratrol suppresses growth of cancer stem-like cells by inhibiting fatty acid synthase. *Breast Cancer Res. Treat.* **130,** 387–398
52. Gnoni, G. V., and Paglialonga, G. (2009) Resveratrol inhibits fatty acid and triacylglycerol synthesis in rat hepatocytes. *Eur. J. Clin. Invest.* **39,** 211–218
53. Picard, F., Kurtev, M., Chung, N., Topark-Ngarm, A., Senawong, T., Machado De Oliveira, R., Leid, M., McBurney, M. W., and Guarente, L. (2004) Sirt1 promotes fat mobilization in white adipocytes by repressing PPAR-γ. *Nature* **429,** 771–776
54. Szkudelska, K., Nogowski, L., and Szkudelski, T. (2009) Resveratrol, a naturally occurring diphenolic compound, affects lipogenesis, lipolysis and the antilipolytic action of insulin in isolated rat adipocytes. *J. Steroid Biochem. Mol. Biol.* **113,** 17–24
55. Mercader, J., Palou, A., and Bonet, M. L. (2011) Resveratrol enhances fatty acid oxidation capacity and reduces resistin and retinol-binding protein 4 expression in white adipocytes. *J. Nutr. Biochem.* **22,** 828–834
56. Berton, G., Mócsai, A., and Lowell, C. A. (2005) Src and Syk kinases. Key regulators of phagocytic cell activation. *Trends Immunol.* **26,** 208–214
57. Su, L., and David, M. (2000) Distinct mechanisms of STAT phosphorylation via the interferon-α/β receptor. Selective inhibition of STAT3 and STAT5 by piceatannol. *J. Biol. Chem.* **275,** 12661–12666
58. Wang, B. H., Lu, Z. X., and Polya, G. M. (1998) Inhibition of eukaryote serine/threonine-specific protein kinases by piceatannol. *Planta Med.* **64,** 195–199
59. Wang, H., and Malbon, C. C. (1999) $G_s\alpha$ repression of adipogenesis via Syk. *J. Biol. Chem.* **274,** 32159–32166
60. Roupe, K. A., Yáñez, J. A., Teng, X. W., and Davies, N. M. (2006) Pharmacokinetics of selected stilbenes. Rhapontigenin, piceatannol, and pinosylvin in rats. *J. Pharm. Pharmacol.* **58,** 1443–1450
61. Yu, C., Shin, Y. G., Chow, A., Li, Y., Kosmeder, J. W., Lee, Y. S., Hirschelman, W. H., Pezzuto, J. M., Mehta, R. G., and van Breemen, R. B. (2002) Human, rat, and mouse metabolism of resveratrol. *Pharm. Res.* **19,** 1907–1914
62. Amri, A., Chaumeil, J. C., Sfar, S., and Charrueau, C. (2012) Administration of resveratrol: what formulation solutions to bioavailability limitations? *J. Controlled Release,* in press
63. Johnson, J. J., Nihal, M., Siddiqui, I. A., Scarlett, C. O., Bailey, H. H., Mukhtar, H., and Ahmad, N. (2011) Enhancing the bioavailability of resveratrol by combining it with piperine. *Mol. Nutr. Food Res.* **55,** 1169–1176
64. Brown, V. A., Patel, K. R., Viskaduraki, M., Crowell, J. A., Perloff, M., Booth, T. D., Vasilinin, G., Sen, A., Schinas, A. M., Piccirilli, G., Brown, K., Steward, W. P., Gescher, A. J., and Brenner, D. E. (2010) Repeat dose study of the cancer chemopreventive agent resveratrol in healthy volunteers. Safety, pharmacokinetics, and effect on the insulin-like growth factor axis. *Cancer Res.* **70,** 9003–9011
65. Geahlen, R. L., and McLaughlin, J. L. (1989) Piceatannol (3,4,3′,5′-tetrahydroxy-trans-stilbene) is a naturally occurring protein-tyrosine kinase inhibitor. *Biochem. Biophys. Res. Commun.* **165,** 241–245
66. Thakkar, K., Geahlen, R. L., and Cushman, M. (1993) Synthesis and protein-tyrosine kinase inhibitory activity of polyhydroxylated stilbene analogs of piceatannol. *J. Med. Chem.* **36,** 2950–2955